Electronic Supplementary Material (ESI) for Lab on a Chip.

Supplementary Information

Toward 3D Printed Microfluidic Artificial Lungs for Respiratory Support

Elyse Fleck,[a,b] Charlise Keck [a,b], Karolina Ryszka [a,b], Andrew Zhang [a,b], Michael Atie [a,b], Sydney Maddox[a,b], and Joseph Potkay [a,b]

Affiliations
[a]ECLS Laboratory, Department of Surgery, University of Michigan, Ann Arbor, MI 48109, USA
[b]VA Ann Arbor Healthcare System, Ann Arbor, MI 48105, USA

Figure S1. Dimensioned SOLIDWORKS rendering of µAL

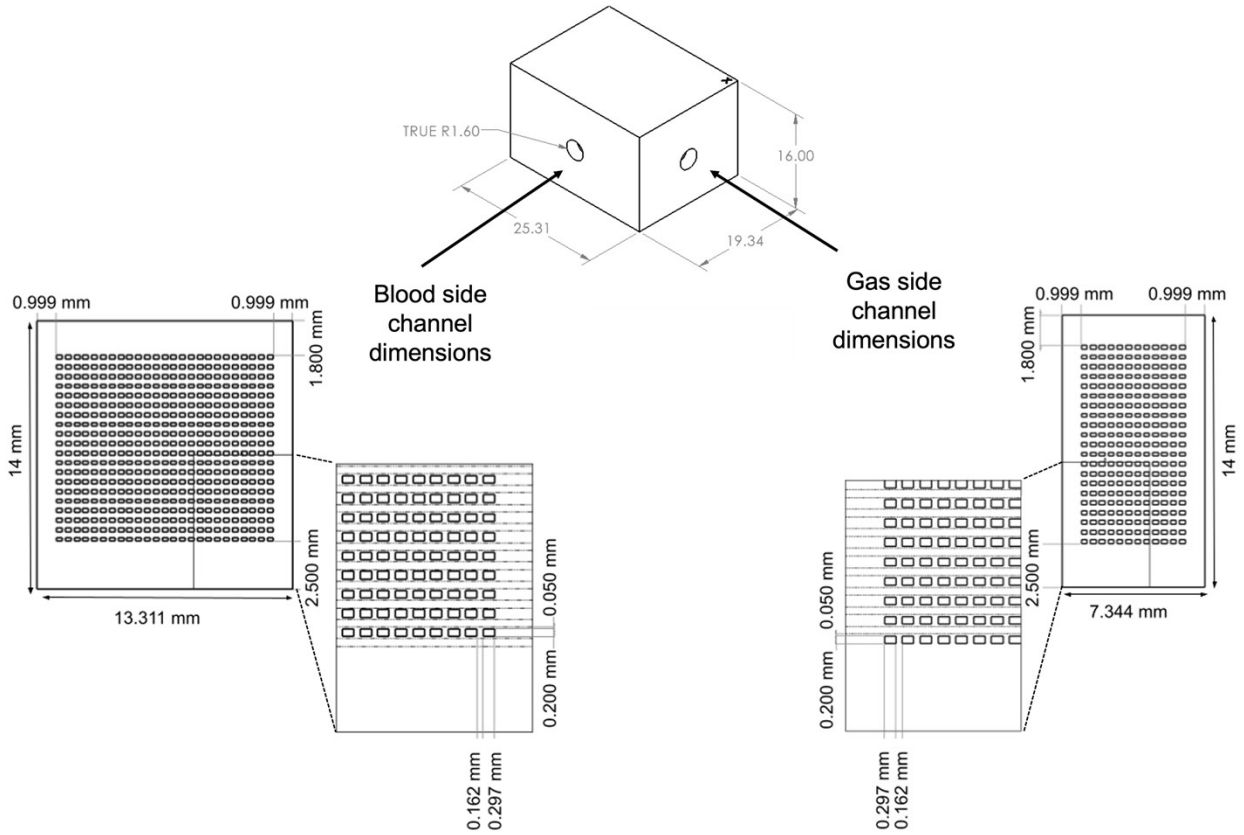

Figure S2. Dimensioned images of internal channels of 3D printed µAL

The image below is a representative photo of the internal structure of the µAL. To determine the actual printed dimensions of the part, n=4 µALs were deconstructed to reveal the channels seen in the image below and imaged with an AM413T Dino-Lite Digital Microscope using DinoCapture 2.0 software (Dunwell Tech, Inc., Torrance, CA, USA; camera resolution was ±3 µm) at 150x magnification. Dimensions were averaged and standard deviations were calculated and are presented in the table. Deviations from the designed dimensions are due to over-curing of channels — an artifact of DLP 3D printing. Additional error may be due to a lack of precision of the equipment where the Dino Lite microscope has a precision of 3 micrometers when using the measurement tool.

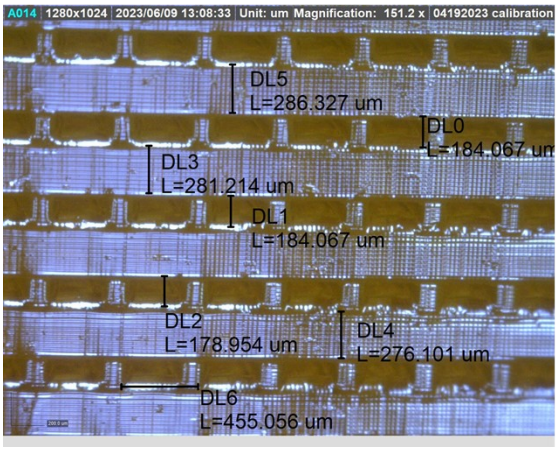

	Designed	Actual
Channel Height	200	171.8 ± 15.4
Membrane + Perpendicular Channel	250	296.3 ± 14.2
Horizontal Spacing	459	444.9 ± 18.1
Membrane Thickness	50	62.2 ± 4.8
Channel Width	297	320.0 ± 17.0
Pillar Width	162	124.1 ± 12.4

Figure S3. MicroCT scans of µAL devices (n=3), plot of percentage of occluded (uncleared) and patent (cleared) channels inside the device (error bars represent standard deviation), and average number (with standard deviation) of occluded and patent channels inside the device.

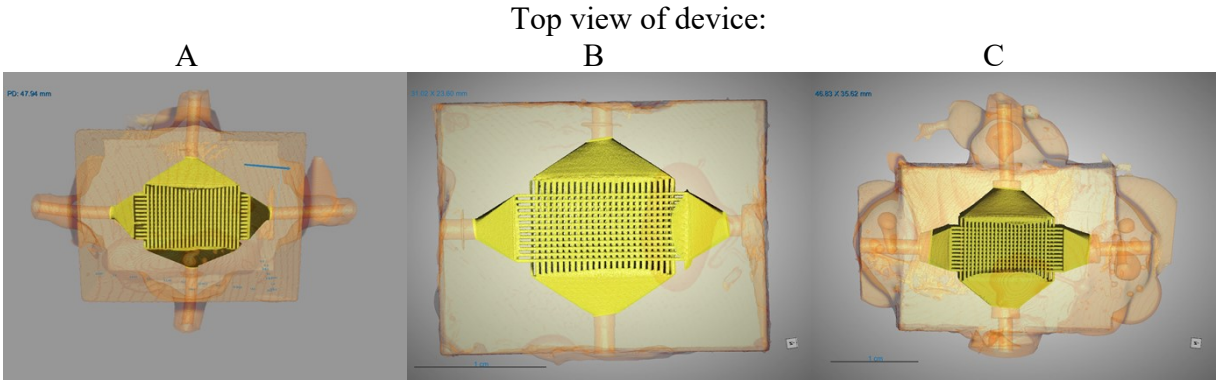

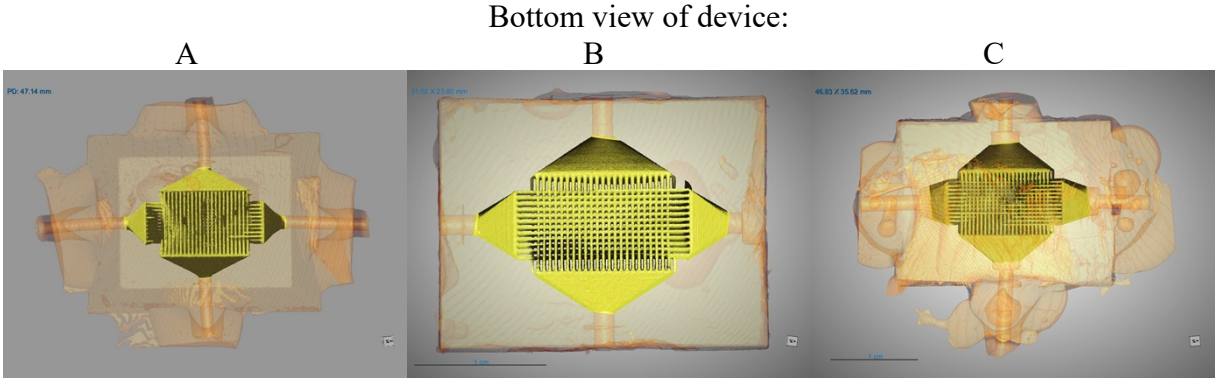

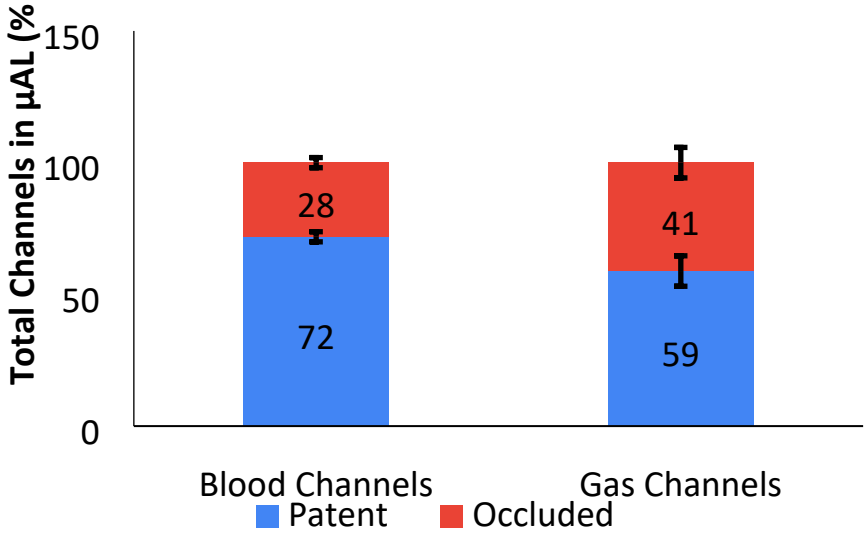

Average count of patent (cleared) and occluded channels inside device (n=3).		
	Blood channels	Gas channels
Patent	359 ± 10	148 ± 15
Occluded	141 ± 10	104 ± 15

Figure S4. Roughness of 3D Printed Parts. The 3D printed microchannels shown below were printed on an Asiga MAX X27 UV DLP printer as an array of micron-scale, rectangular channels ranging from 140 to 40 µm tall (left to right) and membranes ranging from 20 to 100 µm thick (A). The first column of channels (140 µm tall) was sliced open (B) to expose the side walls inside channels for surface roughness imaging (C, D). The roughness (root mean square height), is s_q = 4.9 µm and the roughness on the top and bottom of the channels is s_q = 0.4 µm. *Figure S4a is reproduced from E. Fleck, A. Sunshine, E. DeNatale, C. Keck, A. McCann and J. Potkay, Micromachines, 2021, 12, 1266.*

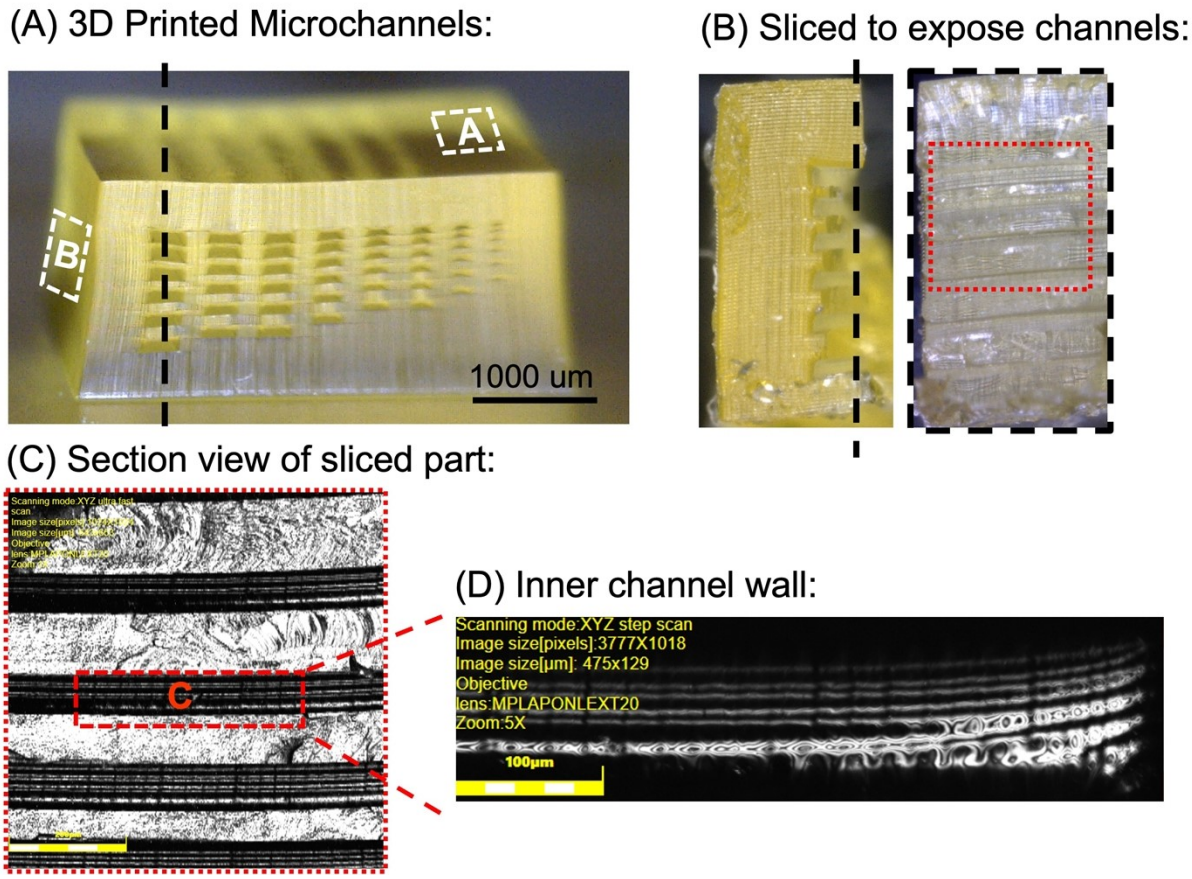

Location	A	B	C
Roughness (µm)	0.387	2.549	4.916

Figure S5. Blood Testing Set Up

Benchtop setup:

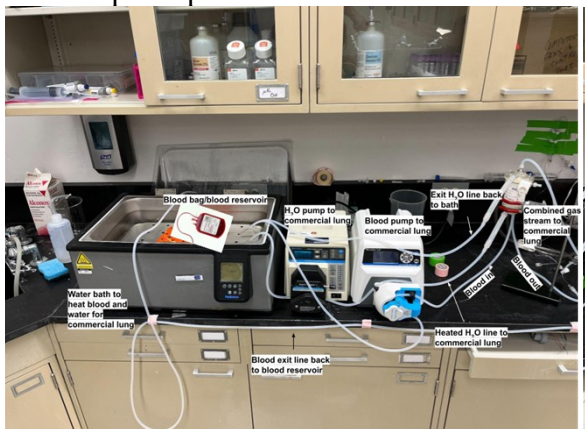

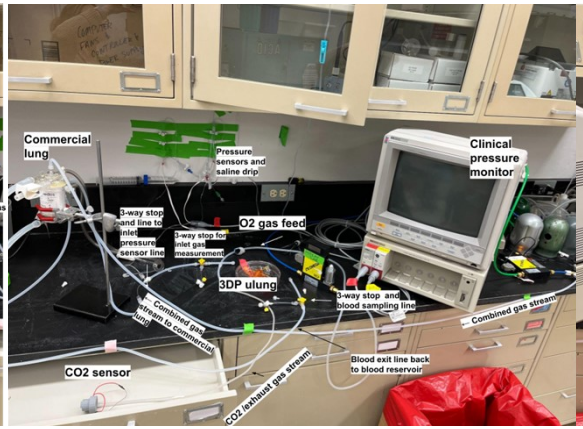

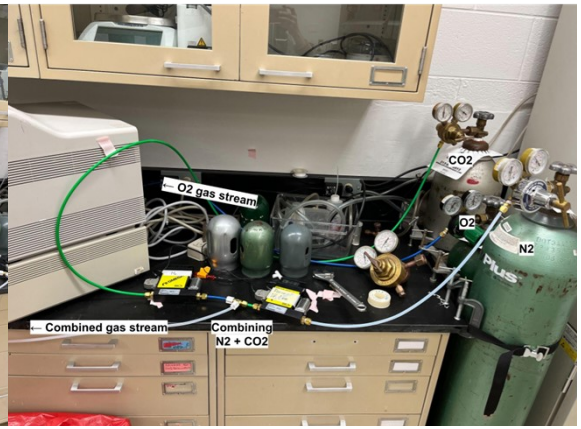

µAL during blood testing:

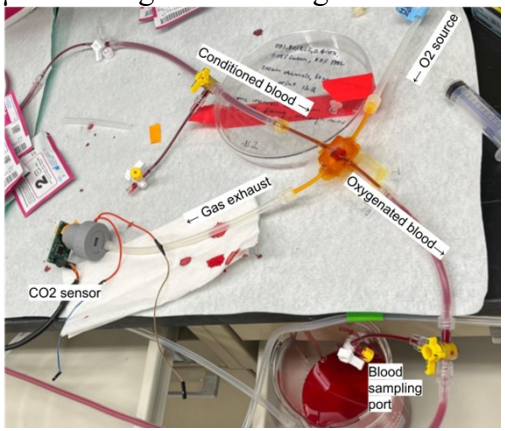

Figure S6. Volume transfer and CO_2 volume transfer versus blood flow for *in vitro* μAL blood tests. In (A), sweep gas to blood flow ratio is 4:1. Blood flow rate for (B) is 5.0 mL/min.

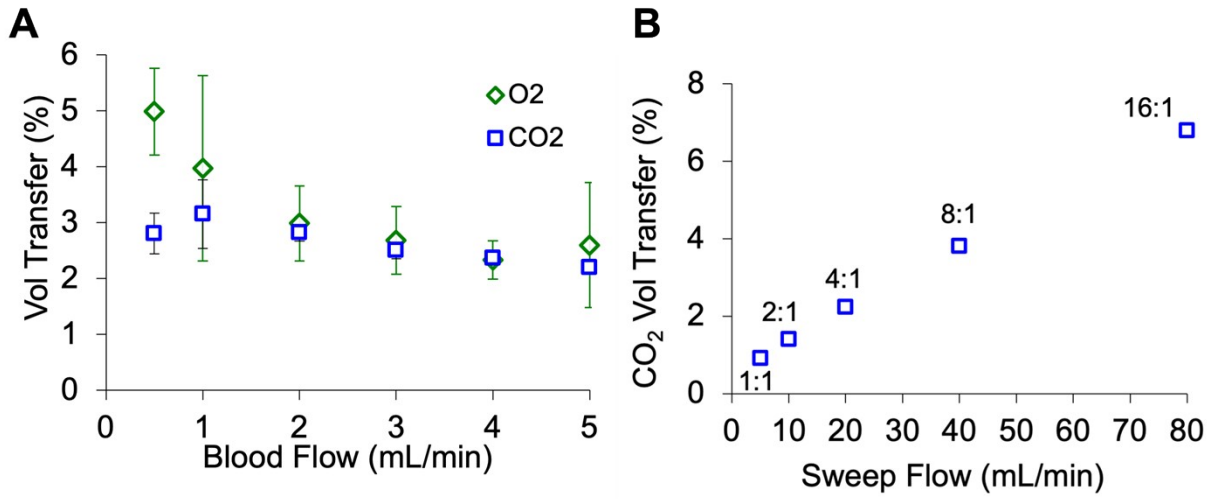

Figure S7. Theory plots for µAL device performance parameters at varying capillary heights. Active device volume is the same as the µAL in the main manuscript (WxLxH = 1.2x0.73x0.94 cm); sweep gas is pure O_2; ratio of channel width to height and channel width to channel spacing is the same as the µAL in the manuscript; gas exchange membrane is 50 µm thick.

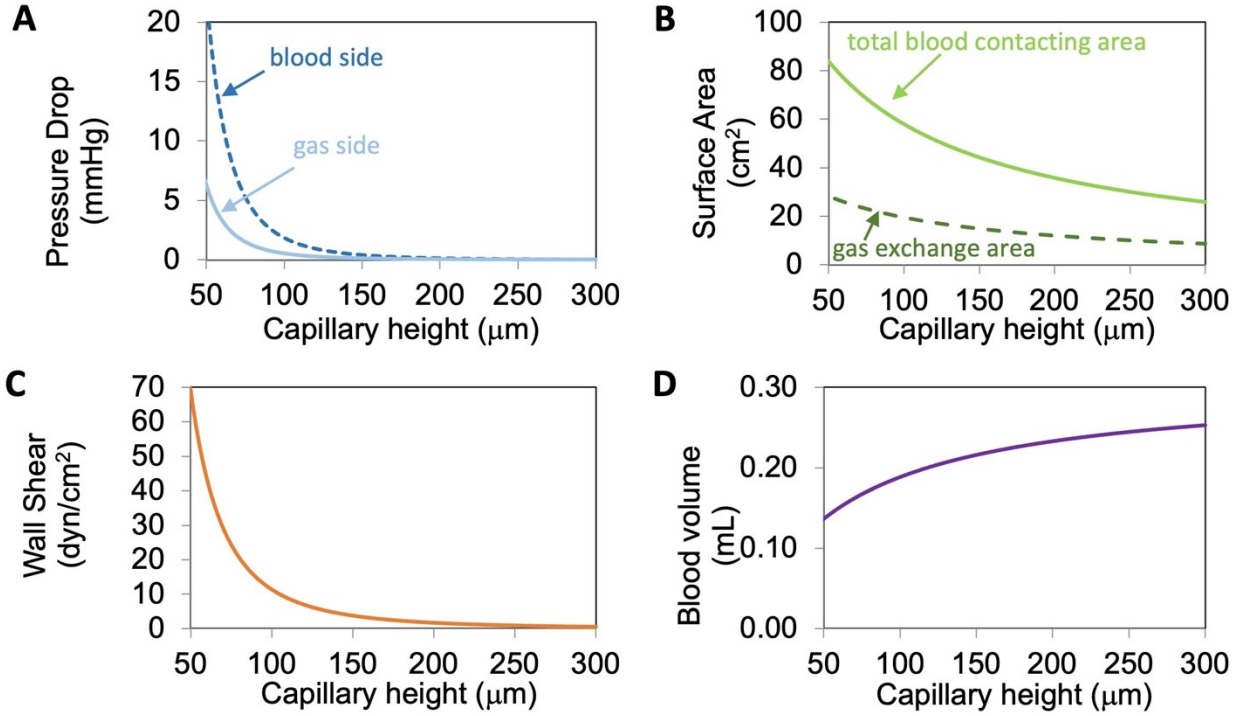

Figure S8. Theory plots for µAL device performance parameters at varying membrane thicknesses. Active device volume is the same as the µAL in the main manuscript (WxLxH = 1.2x0.73x0.94 cm); sweep gas is pure O_2; blood channels are fixed at 200x297x7200 µm (HxWxL).

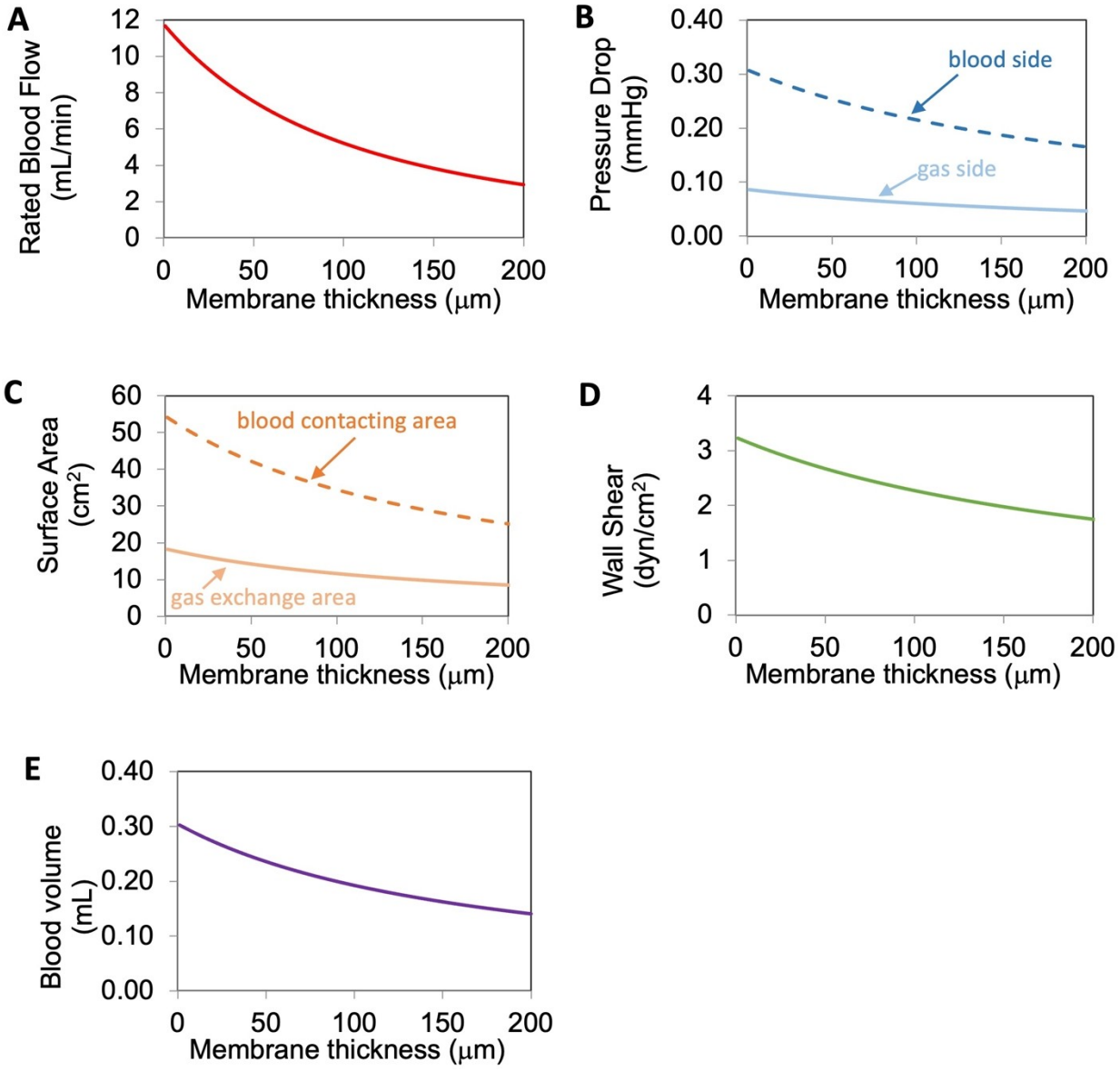

Table S1. Equations used in the mathematical modelling of μAL performance.

Partial pressure of oxygen in blood	$PO2_{B,o} = PO2_G + (PO2_{B,i} - PO2_G)e^{-\frac{A_{C,G}}{Q \cdot S_{B,O2} \cdot R_{D,O2}}}$
$PO2_B$ is the partial pressure of oxygen in blood, the subscripts O, I, and G represent outlet, inlet, and gas phase, δ_M is the membrane thickness, $P_{M,O2}$ is the permeability of the membrane to oxygen, H_C is the artificial capillary height, and $D_{B,O2}$ is the effective diffusivity of oxygen in blood. The $P_{M,O2}$ of PDMS is 3.6×10^{-7} mL-O2·cm^{-1}·min^{-1}·mmHg^{-1}.	
Resistance to oxygen diffusion	$R_{D,O2} = \frac{\delta_M}{P_{M,O2}} + \frac{H_{EFF}}{S_{B,O2} \cdot D_{B,O2}}$
$R_{D,O2}$ depends on membrane thickness (δ_M), channel height (H), membrane permeability to oxygen ($P_{M,O2}$), effective diffusivity of oxygen in blood ($D_{B,O2}$) and $S_{B,O2}$. Normal human blood has a $D_{B,O2}$ of approximately 1.4×10^{-6} cm^2/s[1]. In normal human blood, $S_{B,O2}$ is a constant, at approximately 7.9×10^{-4} mL-O$_2$·mL-blood^{-1}·mmHg^{-1}[1]. H_{EFF} is the effective height, i.e. average distance, that oxygen must travel in blood to bind with hemoglobin. In single sided diffusion, $H_{EFF} = H_C/2$, where H_C is the artificial capillary height. In double sided diffusion, $H_{EFF} = H_C/4$. For double sided diffusion, $R_{D,O2}$ is the parallel combination of the resistance to diffusion through the top membrane and resistance through the bottom membrane.	
Oxygen saturation in blood (Hill equation)[2]	$SO_2 = \frac{\left(PO_2/P_{50}\right)^n}{1 + \left(PO_2/P_{50}\right)^n}$
SO_2 is the oxygen saturation of blood, n is a constant (≈2.7 for human blood), and P_{50} is the PO_2 at which SO_2=50% (≈27 mmHg for normal human blood).	
Rated blood flow	$Q_R = \frac{A_{c,g}}{S_{B,O2} \cdot R_{D,O2} \cdot ln\left(\frac{PO2_{B,i} - PO2_G}{PO2_{B,o} - PO2_G}\right)}$
$A_{c,g}$ is the capillary gas exchange area, and $PO2_{B,i}$, $PO2_{B,O}$ and $PO2_G$ are the partial pressures of oxygen in the blood entering and exiting capillaries and in the sweep gas, respectively. For pure oxygen, $PO2_G$ was estimated as 760 mmHg. For normal human blood, $PO2_{B,I}$ and $PO2_{B,O}$ are 36.4 mmHg and 79.2 mmHg, corresponding to SO_2 values of 70% and 95%, respectively.	
Blood viscosity[3,4]	$\mu = \mu_P\{1 + 0.025 \cdot HCT + (7.35 * 10^{-4})HCT^2\}$
μ_P is bovine plasma viscosity (1.72 cP)[REF] and HCT is the blood hematocrit.	
Pressure drop	$\Delta P = \frac{12 \cdot \mu \cdot L}{H \cdot W^3 \cdot \left(1 - \frac{0.63 \cdot H}{W}\right)} Q$
L, H, and W are the channel dimensions and Q is flow. For the case of the array of N_C parallel artificial capillaries presented here, flow is approximately evenly divided into all N_C artificial capillaries and the total pressure drop is the pressure drop of a single channel divided by N_C.	
Shear stress	$\tau_W = 6 \cdot \mu \cdot v \cdot H^{-1}$
τ_w is average flow velocity ($v = Q \cdot W^{-1} \cdot H^{-1}$), and H is the height of each capillary [5]. In the human vascular system, shear stress ranges between 10 and 70 dyn/cm^2 in arteries and between 1 and 6 dyn/cm^2 in veins [6].	

[1] J. A. Potkay, Biomed Microdevices, 2013, 15, 397–406.
[2] A. V. Hill, The Journal of Physiology, 1910, 40, i--vii.
[3] E. W. Errill, Physiological Reviews, 1969, 49, 863–888.
[4] A. J. Thompson, L. H. Marks, M. J. Goudie, A. Rojas-Pena, H. Handa and J. A. Potkay, Biomicrofluidics, 2017, 11, 024113.
[5] R. G. Bacabac, T. H. Smit, S. C. Cowin, J. J. W. A. Van Loon, F. T. M. Nieuwstadt, R. Heethaar and J. Klein-Nulend, *Journal of Biomechanics*, 2005, **38**, 159–167.
[6] A. M. Malek, S. L. Alper and S. Izumo, *JAMA*, 1999, **282**, 2035–2042.

Figure S9. Oxygen hemoglobin dissociation curve. Experimental data (circles) fitted to the Hill equation (solid line). The oxygen-hemoglobin dissociation curve for normal human blood is shown as a dashed line. The average effective oxygen solubility ($S_{B,O2}$) and diffusivity ($D_{B,O2}$) for the experimental data were calculated over the range of average inlet blood PO_2 (50.2 mmHg) to the average outlet blood PO_2 (87.5 mmHg) resulting in $S_{B,O2} = 9.3x10^{-4}$ mL O2·mL^{-1}·mmHg^{-1} and $D_{B,O2} = 7.3x10^{-7}$ cm^2·s^{-1}.

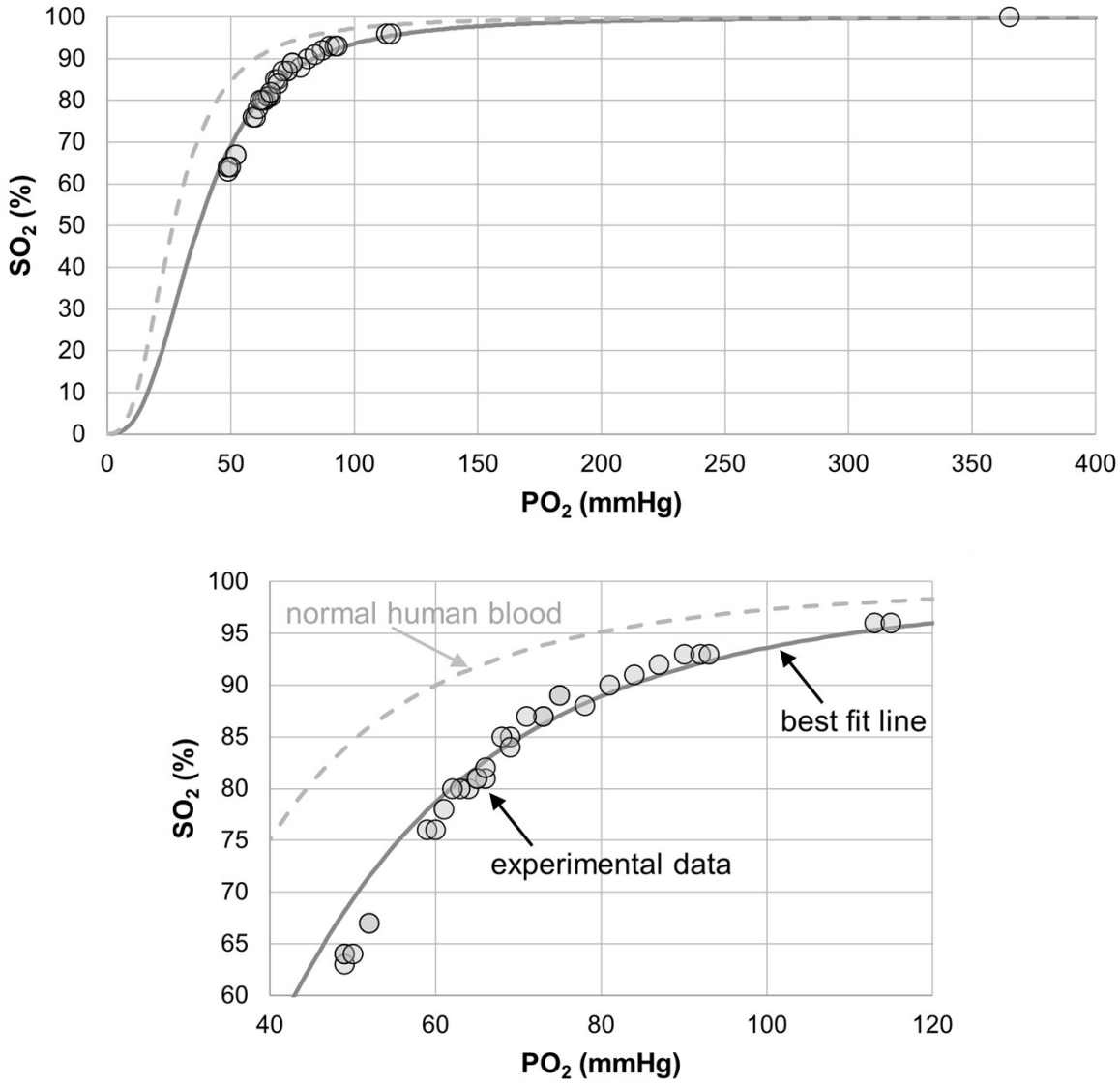

Figure S10. Clearing circuit with ethanol and food dye to visualize patency of microchannels during post-processing of the 3D printed µAL.